

# Supporting Information

## Direct Synthesis of Bulk Boron-Doped Graphitic Carbon

Nicholas P. Stadie, Emanuel Billeter, Laura Piveteau, Kostiantyn V. Kravchyk, Max Döbeli, and Maksym V. Kovalenko

### Contents:

Tables S1-S3. Acquisition parameters for  $^{11}\text{B}$  and  $^{13}\text{C}$  NMR experiments

Figure S1. Photographs of precursors and  $\text{BC}_3'$  product

Figure S2.  $^{13}\text{C}$  MAS NMR spectrum of  $\text{BC}_3'$

Figure S3. Raman spectroscopy of reference materials

Figure S4. XRD comparison between tiled  $\text{BC}_3'$  and  $\text{BC}_3'$  (this work)

Figure S5. SEM comparison between tiled  $\text{BC}_3'$  and  $\text{BC}_3'$  (this work)

Figure S6. Raman spectroscopy comparison between tiled  $\text{BC}_3'$  and  $\text{BC}_3'$  (this work)

Figure S7. Raman spectroscopy analysis of various  $\text{BC}_3'$  materials

Figure S8.  $^{11}\text{B}$  MAS NMR comparison between tiled  $\text{BC}_3'$  and  $\text{BC}_3'$  (this work)

Figures S9-S10. ERDA comparison between tiled  $\text{BC}_3'$  and  $\text{BC}_3'$  (this work)

**Table S1.** Acquisition parameters for  $^{11}\text{B}$  MQMAS NMR (Figure 5)

Magnetic Field (T)	16.4
Temperature (K)	298
Rotor Diameter (mm)	2.5
Pulse Sequence	mp3qdfs (Bruker)
Number of Scans	1664
Recycle Delay (s)	0.6
Spectral Width (kHz)	Direct Dimension: 100 Indirect Dimension: 125
Spinning Frequency (kHz)	20
Acquisition Length (points)	Direct Dimension: 1024 Indirect Dimension: 256
Rotor Cycles for Synchronization	40
Indirect Dimension Increment ( $\mu\text{s}$ )	8.0
Split- $t_1$ Increment ( $\mu\text{s}$ )	6.2
$^{11}\text{B}$ Excitation Pulse Width [ $\pi/2$ ] ( $\mu\text{s}$ )	4.5
Double Frequency Sweep Length ( $\mu\text{s}$ )	12.5
$^{11}\text{B}$ Selective Pulse Width [ $\pi$ ] ( $\mu\text{s}$ )	42

**Table S2.** Acquisition parameters for  $^{11}\text{B}$  MAS NMR (Figure S7)

Magnetic Field (T)	16.4
Temperature (K)	298
Rotor Diameter (mm)	2.5
Pulse Sequence	hahnecho (Bruker)
Number of Scans	304
Recycle Delay (s)	1
Spectral Width (kHz)	100
Spinning Frequency (kHz)	20
Acquisition Length (points)	2048
$^{11}\text{B}$ $90^\circ$ Pulse Width [ $\pi/2$ ] ( $\mu\text{s}$ )	22

**Table S3.** Acquisition parameters for  $^{13}\text{C}$  MAS NMR (Figure S1)

Magnetic Field (T)	16.4
Temperature (K)	298
Rotor Diameter (mm)	2.5
Pulse Sequence	zg30 (Bruker)
Number of Scans	936
Recycle Delay (s)	120
Spectral Width (kHz)	178.6
Spinning Frequency (kHz)	20
Acquisition Length (points)	2048
$^{13}\text{C}$ $90^\circ$ Pulse Width [ $\pi/2$ ] ( $\mu\text{s}$ )	3.4

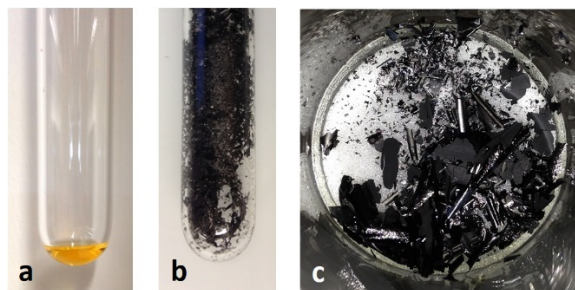


**Figure S1.** Photographs of (a) precursor solution ( $\text{BBr}_3$  and  $\text{C}_6\text{H}_6$ ), (b) as-carbonized  $\text{BC}_3'$ , and (c) collected/washed  $\text{BC}_3'$  after direct synthesis for 1 h at  $800\text{ }^\circ\text{C}$ .

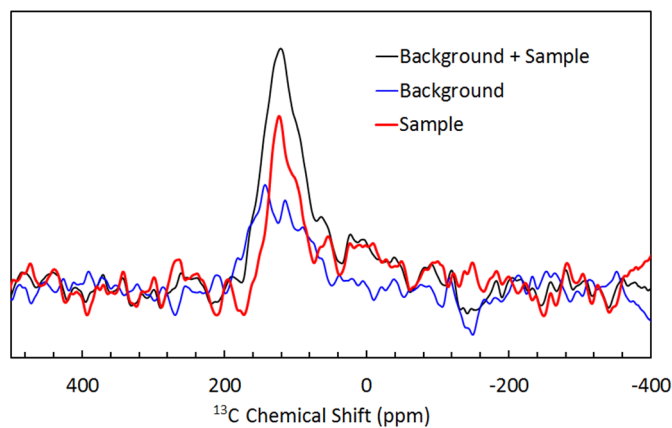


**Figure S2.**  $^{13}\text{C}$  MAS NMR spectrum of directly-synthesized  $\text{BC}_3'$  deconstructed to show the background contribution from the probe.

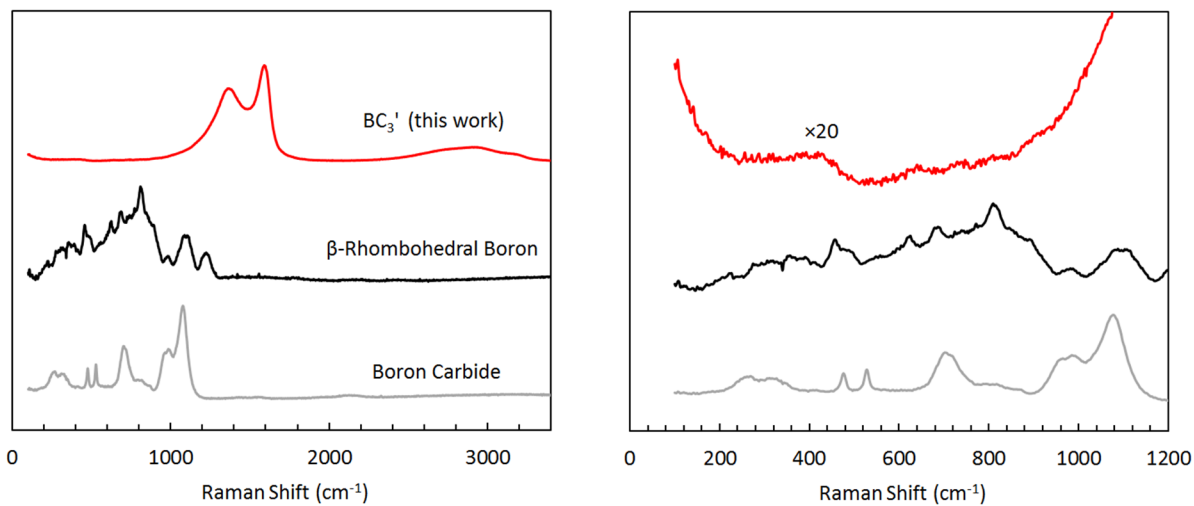


**Figure S3.** Raman spectra of boron carbide and  $\beta$ -rhombohedral boron reference samples in comparison to directly-synthesized  $\text{BC}_3'$ .

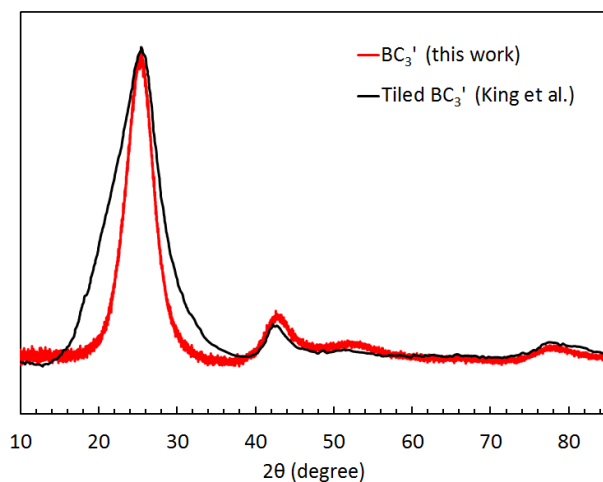


**Figure S4.** XRD pattern of tiled BC<sub>3</sub>'<sup>[S1]</sup> in comparison to directly-synthesized BC<sub>3</sub>', both synthesized at 800 °C under “optimal” heating ramps (6 °C/h and 60 °C/h, respectively).

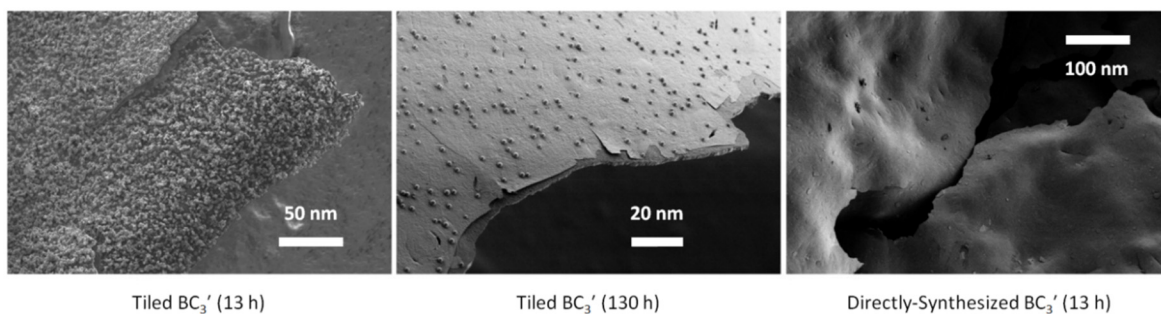


**Figure S5.** SEM micrographs of tiled BC<sub>3</sub>' (obtained after 13 h or 130 h, this work) in comparison to directly-synthesized BC<sub>3</sub>' (obtained after 13 h, this work).

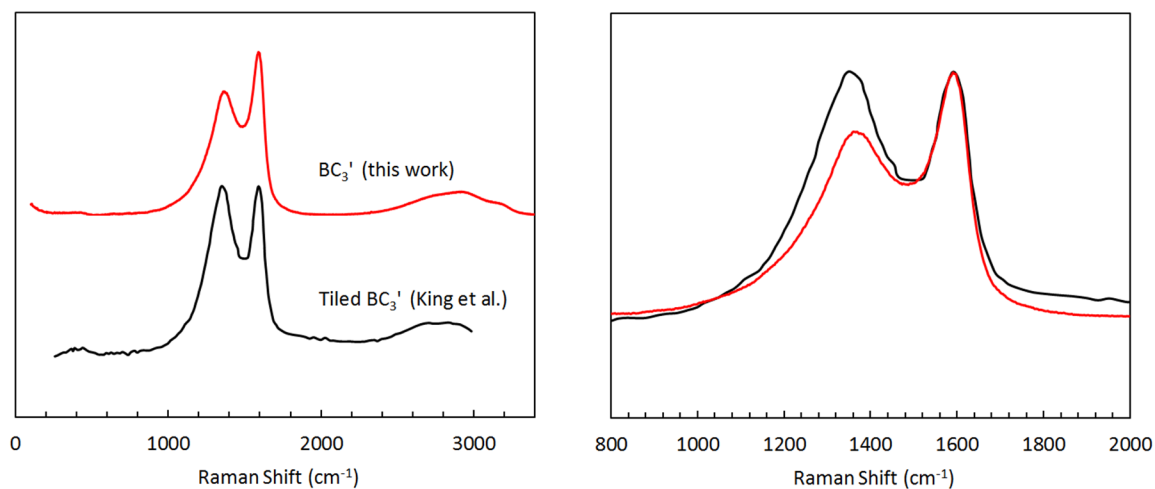


**Figure S6.** Raman spectrum of tiled BC<sub>3</sub>'<sup>[S1]</sup> in comparison to directly-synthesized BC<sub>3</sub>'.

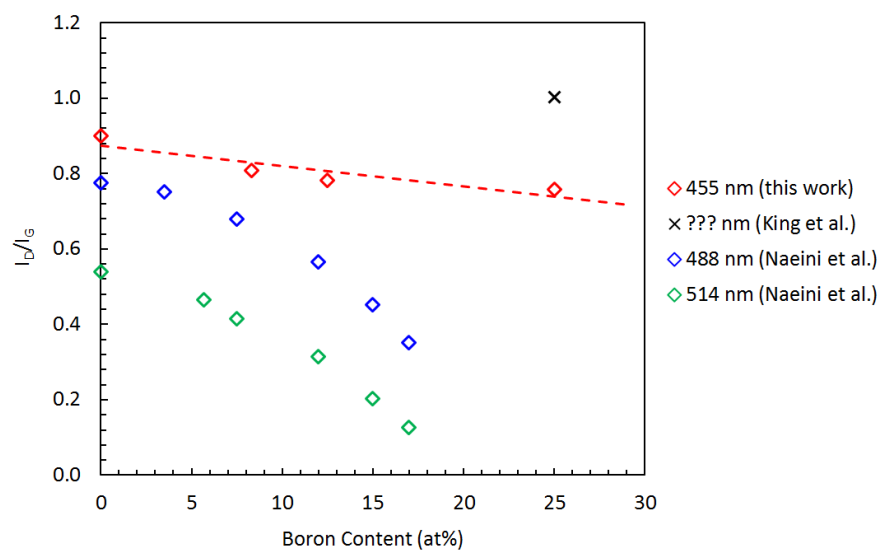


**Figure S7.** Raman spectroscopy analysis of the  $I_D/I_G$  ratio as a function of boron content and excitation wavelength in thin-film  $BC_x'$  [S3] in comparison to directly-synthesized  $BC_x'$ .

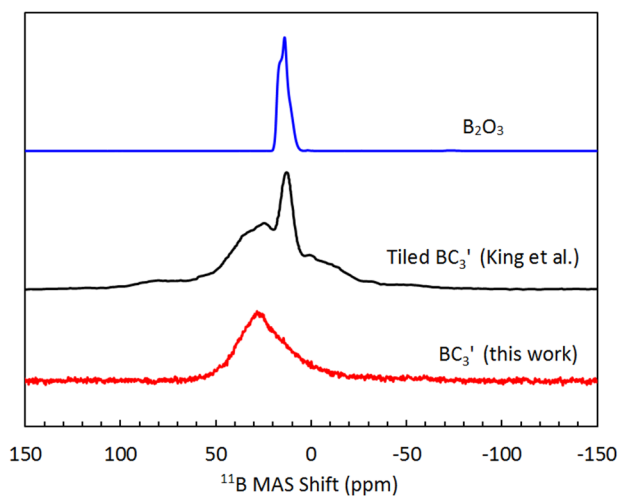


**Figure S8.**  $^{11}\text{B}$  MAS NMR spectra of boron trioxide ( $B_2O_3$ ) [S2] and tiled  $BC_3'$  [S1] in comparison to directly-synthesized  $BC_3'$  (this work).

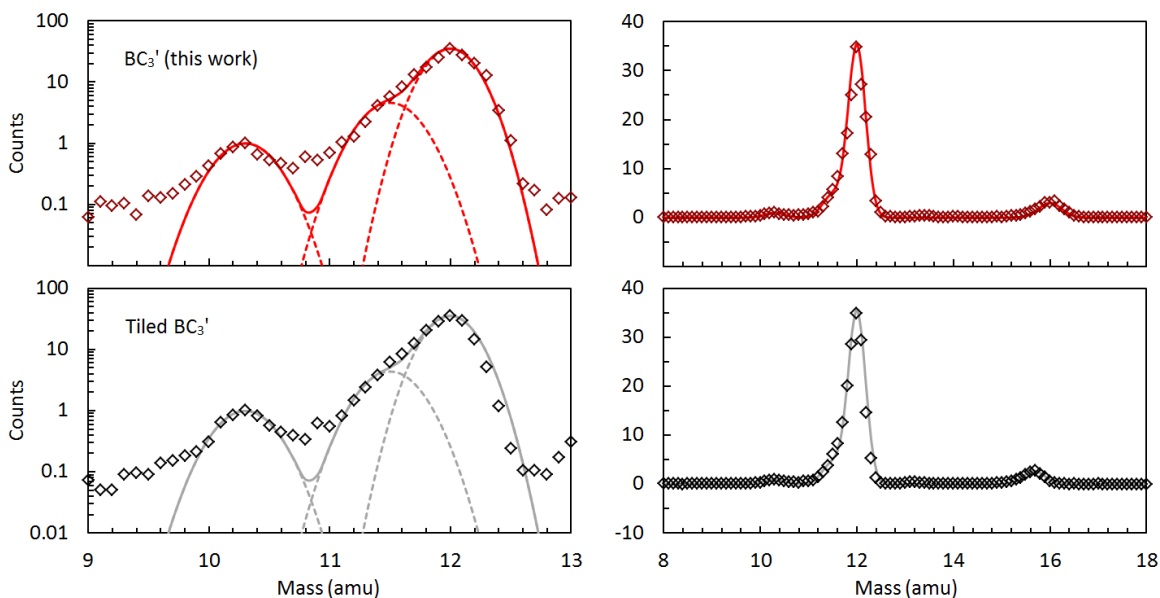


**Figure S9.** Representative ERDA spectrum of tiled  $\text{BC}_3'$  (synthesized herein, following the route described elsewhere<sup>[S1]</sup>) in comparison to directly-synthesized  $\text{BC}_3'$  (this work).

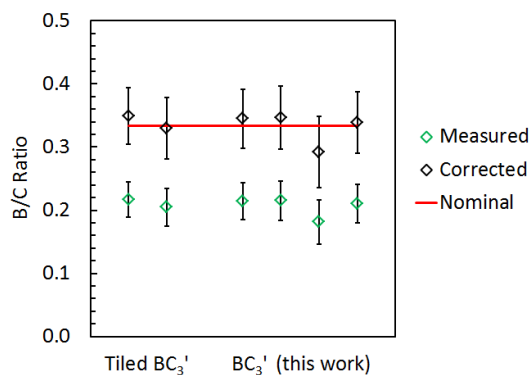


**Figure S10.** ERDA composition of tiled  $\text{BC}_3'$  and directly-synthesized  $\text{BC}_3'$  (as in Figure S8).

### Supporting References:

- (S1) King, T. C.; Matthews, P. D.; Glass, H.; Cormack, J. A.; Holgado, J. P.; Leskes, M.; Griffin, J. M.; Scherman, O. A.; Barker, P. D.; Grey, C. P.; Dutton, S. E.; Lambert, R. M.; Tustin, G.; Alavi, A.; Wright, D. S., Theory and Practice: Bulk Synthesis of  $\text{C}_3\text{B}$  and its  $\text{H}_2$ - and Li-Storage Capacity. *Angew. Chem. Int. Ed.* **2015**, *54*, 1-6.
- (S2) Kroeker, S.; Stebbins, J. F., Three-Coordinated Boron-11 Chemical Shifts in Borates. *Inorg. Chem.* **2001**, *40* (24), 6239-6246.
- (S3) Naeini, J. G.; Way, B. M.; Dahn, J. R.; Irwin, J. C., Raman scattering from boron-substituted carbon films. *Phys. Rev. B* **1996**, *54* (1), 144-151.